

PREDICTING LUMBER TENSILE STIFFNESS AND STRENGTH WITH LOCAL GRAIN ANGLE MEASUREMENTS AND FAILURE ANALYSIS

S. M. Cramer

Assistant Professor of Civil and Environmental Engineering
University of Wisconsin
Madison, Wisconsin 53706

and

K. A. McDonald

Research Wood Scientist
USDA, Forest Service
Forest Products Laboratory¹
Madison, Wisconsin 53705-2398

(Received October 1988)

ABSTRACT

A mechanistic model is presented for predicting the tensile stiffness and strength of 2 by 4 lumber boards containing a single major face knot. The primary inputs to the model are local grain angle maps for each wide face of a board and estimates of average clear-wood properties. The grain angle maps were obtained through electrical scanning of board surfaces and represented the in-plane orientation of the wood fibers. Out-of-plane dive angles were not considered. The model simulates the failure process that occurs within lumber subject to tension and thereby provides insight to, and understanding of, the failure of wood with defects. The model is devoid of empirical adjustment factors, and it has produced tensile strength predictions that correlate with measured strengths by a correlation coefficient of 0.86 and an average absolute error of 12%. It is hoped that insight gained through use of this model will provide a foundation for improvements in lumber grading.

Keywords: Lumber tensile strength, fracture, finite element.

INTRODUCTION

Improved methods to define and manage lumber strength and stiffness variability are needed in anticipation of new reliability-based design procedures, new markets, and new applications for structural lumber. Reliability-based design procedures reward designs that use structural products with known and controlled variability in strength and stiffness. New markets and new applications for structural lumber products will likely appear when we are able to predict the strength of lumber members more accurately and confidently.

The two most significant growth characteristics affecting lumber strength are knots and variations in grain orientation. Knots present a weakened zone in lumber, which causes higher stresses in adjacent material. Associated with knots or occurring separately are wood fibers with grain angles that are not parallel to

¹ The Forest Products Laboratory is maintained in cooperation with the University of Wisconsin. This article was written and prepared by U.S. Government employees on official time, and it is therefore in the public domain and not subject to copyright.

the longitudinal axis of a board. The extreme imbalance of strength properties that are parallel to grain, as opposed to perpendicular, makes grain orientation critical in determining wood strength. The ratio of clear-wood tensile strengths parallel to perpendicular to grain can be 40 to 1. According to Hankinson's formula, a small, clear tension specimen would experience more than 20% loss in strength with as little as 5 degrees of grain angle. A similar effect likely occurs locally in the grain angle deviations around knots when lumber is loaded in tension or bending. Although knots can be detected and measured visually, the measurement of grain angle variations has been difficult until recently.

Our primary objective has been to develop a theoretical model to predict the ultimate tensile strength of lumber members. Rational modeling of the behavioral characteristics of lumber subject to tensile load is an important secondary objective. This secondary objective includes modeling the local fracture process that occurs in lumber prior to ultimate load. We have purposely avoided empirical adjustment factors and have concentrated on mechanistic approaches to these objectives. The finite element method with fracture mechanics considerations forms the basis of the model.

The primary inputs to the model are local surface grain angle maps covering the portion of board length that includes a critical wide-face knot. Our research hypothesis was that these maps, combined with estimates of wood properties, would provide sufficient information for a general theoretical model for predicting the tensile strength of individual boards more accurately than has been possible to date.

BACKGROUND

New strength prediction methods

Although the need for improved methods to predict lumber strength has been recognized (ASCE 1984), the actual development of new methods has been hampered by the complexity of lumber material and the inability to measure and account for the variability that occurs within lumber members.

Pearson (1974) modeled the effect of a knot in a tension member by using fracture mechanics concepts and an equivalent transverse crack to represent the heterogeneity presented by knots. Pearson found a strong relationship between loads necessary to cause major fracture in knot-containing specimens and specimens with artificial transverse cracks that were sized to simulate the effect of a knot. Boatright and Garrett (1979) reexamined Pearson's work with specimens that contained greater grain distortion around knots. They found equivalent crack length was not as good a predictor of bending strength as had been indicated in Pearson's experiments.

Both Green (1945) and Tang (1984) explored theoretical elasticity solutions to predict the stress concentration caused by knots. In both studies, only limited results were given since the closed form solutions involved lengthy and tedious calculation, which cannot be easily adapted for practical use. Grain deviations were neglected to make the solution tractable.

Studies were conducted at Colorado State University on the tension behavior of lumber (Anthony 1986; Cramer 1981; Cramer and Goodman 1986; Dabholkar 1980; Pellicane 1980; Petterson and Bodig 1983; Phillips et al. 1981; Pugel 1980,

1986; Zandbergs and Smith 1988). These studies included experimental testing and computer-aided modeling of lumber specimens subject to tension. The studies strongly influenced the model development presented in this paper. Grain deviations associated with knots were predicted and simulated assuming similarity with two-dimensional laminar fluid flow around an elliptical obstruction. This modeling technique is called the flow-grain analogy and was verified by microscopy for a limited sample of boards. In the absence of a means to easily measure actual grain angle patterns, the flow-grain analogy provides a very good first approximation to such patterns. However, the laminar fluid flow theory, which forms the basis of the analogy, clearly does not address many unpredictable growth situations that influence grain patterns around knots.

Recently, Bechtel and Allen (1987) disclosed an empirical method that predicts tensile strength based upon measured local grain angles for a selected lumber population. High correlations between predicted and measured strengths indicate that the approach holds promise. However, the empirical nature of the work and initial sample size indicate a need for further testing, calibration, and verification.

Measuring local grain angle

Measuring the direction of the fibers in wood has long been important to strength prediction. The term "slope of grain" relates the general fiber direction to the edges of a piece. Slope of grain is usually expressed by the ratio between a 1-inch deviation of the grain from the edge or long axis of the piece and the distance in inches within which this deviation occurs. This slope can also be expressed as an angle, which is more appropriate for the local grain deviation measurements around in-grown defects, such as knots, and is of primary interest to our objectives.

Traditionally, the slope of grain has been measured using one of several visual methods (Anderson and Koehler 1955; Koehler 1955). These methods, such as scribing and free-flowing ink, are not practical for establishing local grain angle maps for the strength prediction method presented in this paper.

Automated, nondestructive grain angle measurements have been possible since 1977 (McLauchlan and Kusec 1978). Research has shown that the automated grain angle measuring equipment has the ability to accurately measure local grain direction around knots and along the edges of lumber pieces (McDonald and Bendtsen 1986; Soest 1987). These capabilities allow rapid assessment of the unique grain angle characteristics of an individual board, and, in so doing, provide additional incentive to develop a theoretical model to predict the ultimate tensile strength of lumber members.





SCANNING AND TENSION TESTS OF LUMBER 2 BY 4'S

Selection of lumber for testing

As local grain angle measurements and strength predictions are unique for a board, a testing program was necessary for applying and verifying the theoretical model. Strength analysis cannot proceed until grain angle data are gathered.

Two-by-four structural lumber members of two important species, Douglas-fir and Southern Pine, were selected from No. 2 on-grade, 8-ft material. The objective was to limit the selections to a single major knot type in the central area between the tension grips of the tensile testing machine. Four single-knot configuration

TABLE 1. *Knot configuration types.*

Knot type	Cross section view	Number of specimens	
		Douglas-fir	Southern Pine
Centerline (C)		2	1
Off center (O-C)		0	4
Edge with complete knot on one wide face (E-1)		1	3
Edge with knot on edge of each wide face (E-2)		0	3

types were selected for this study (Table 1). They were centerline knots (C), off-center knots (O-C), and two edge-knot types (E-1, E-2). The centerline knot configuration was restricted to those knots with equal (within 1/2-in.) distance between the knot boundary and board edges. One edge-knot configuration (E-1) consisted of the knot boundary touching or overlapping the board edge on one wide face only, with the knot center located within both wide faces. A triangle of clear wood between the knot boundary and the board edge is visible in the cross section of a board with this knot type. The other edge-knot configuration (E-2) consisted of the knot boundary intersecting the board edge on both wide faces. Off-center knots were exclusive of the centerline or edge-knot descriptions.

All specimens were selected so that each knot type was the only major characteristic within the center 2 ft of the 8-ft length. The 3 ft at each end of each specimen did not contain any strength-reducing characteristics visually estimated to be more significant than the selected knot types.

Scanning of lumber

Each specimen was scanned using a 3/4-in.-diameter rotating head in the Metriguard 510 Slope-of-Grain Indicator.² This grain angle measuring device, originally designed to measure slope of grain for automatic lumber grading, gives the grain angle in degrees with respect to the longitudinal axis of the lumber specimen scanned. The grain angle reading is based on the dielectric constant of wood being greater along the direction of the wood fibers than it is across the grain under the scan head surface (McLauchlan et al. 1973). Optimal grain angle resolution has been obtained with readings taken as close as 1/8 in. apart (McDonald et al. 1987). This device measures the surface grain angle resulting from the projection of the angle of the fibers on the board surface. Significant out-of-plane dive angles can also occur, but these were not measured in our study. We hypothesized that surface angles would provide a good first approximation to the board grain angle map.

Twenty-nine scans were made every 1/8 in. across both wide faces of each 2 by 4 specimen. Each scan line was 20 in. long, with the selected knot located approximately midway along that length. Positive and negative grain angle measurements were recorded every 1/8 in. along each scanline in a manner that ensured accurate measurements at repeatable locations along and across the scanned area. The representative scan layout is shown in Fig. 1. The location of each data point is considered to be at the center of the rotating scanning head. Zero grain angle

² The use of trade or firm names in this publication is for reader information and does not imply endorsement by the U.S. Department of Agriculture of any product or service.

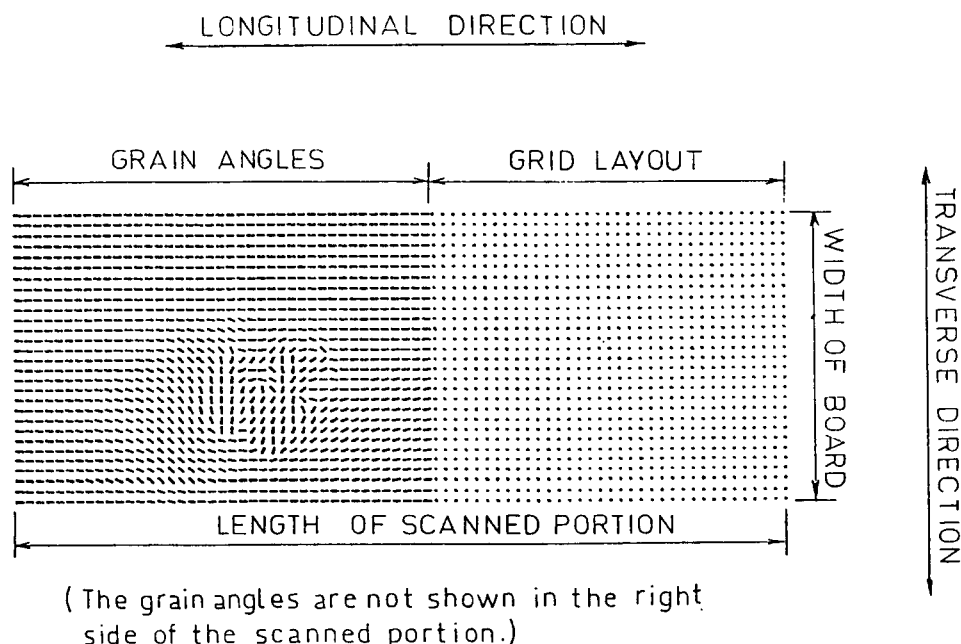


FIG. 1. Grain angle scan layout.

is obtained when the wood fibers in the scanned area are aligned parallel to the longitudinal axis of the specimen (or at least in the same direction as the calibration block when the device is set to zero). A positive angle is a grain deviation in the clockwise direction from the longitudinal axis, and a negative angle, a counter-clockwise deviation.

Full-scale tension tests

Following conditioning to 12% equilibrium moisture content, each 8-ft, 2 by 4 specimen was failed in tension using the Forest Products Laboratory hydraulic tension machine. Fiberglass matting was epoxied onto the wide surfaces of the grip area of each specimen to add strength in the gripping region and to improve the friction between the wood and the tension grip surfaces. Each grip was moved to within 30 in. of the other, to grip approximately 30 in. of the end of each specimen.

Hydraulic grip pressure on the board ends ranged from 1,200 to 1,800 lb/in.² and caused noticeable compression, but not severe crushing. Tensile load was applied under displacement control at a strain rate of approximately 0.0005 in./in.-min. This rate is consistent with recommended average strain rates in ASTM D 198 (1987a). All board failures were associated with the selected knot and were not associated with possible grip-induced stresses.

During initial loading in the tension tests, displacement measurements for calculating an apparent longitudinal *E* (Young's modulus) of the region including the knot were obtained using a clamp arrangement and two linear variable differential transducers (LVDT) mounted on each specimen over a 24-in. span. The extensometer was removed prior to failure to avoid damage.

Tests on small clear-wood specimens

Tests on small clear-wood specimens were conducted to determine the average properties of each 2 by 4. These tests measured density, longitudinal modulus of elasticity, tensile strength perpendicular to grain, and shear strength parallel to grain. Two small clear specimens were manufactured from unfailed portions of each 2 by 4 for each test. Whenever possible, the tests followed the guidelines in ASTM D 143 (1987b) for the testing of small clear specimens.

STRENGTH PREDICTION MODEL*Model capabilities and limitations*

The measured map of grain angles for an individual board has been incorporated into a finite element and fracture mechanics model developed in this research. This model, embodied in the Grain Angle Strength Prediction Program (GASPP), uses the measured local grain angles and constructs a two-dimensional mathematical representation (finite element mesh) of a selected length of board. The construction includes automated locating and sizing of single knots solely from the grain angle data. The board is separated into discrete, small finite elements that possess the assigned grain angle and property characteristics corresponding to the element location within the actual board.

The mathematical representation is analyzed with a special purpose finite element and fracture mechanics algorithm developed as part of this work. This algorithm computes the stress state within each element and computes stress intensity factors for cracks. Stress conditions are assessed for severity based upon failure and fracture criteria built into the algorithm.

Strength and failure mechanisms may be predicted by applying the algorithm in a stepwise fashion by which load causing local fracture is computed. Predicted fracture is accommodated by inserting a crack in the appropriate location within the mesh and reanalyzing—once again computing the load to cause the next occurrence of local fracture. The peak load realized by this stepwise procedure is defined as the predicted strength.

Required input and property data

The GASPP model requires the following general input:

1. Measured local grain angle data set
2. Board length and width
3. Finite element mesh fineness parameters
4. Mesh load and restraint conditions
5. Average clear-wood properties, including
 - a. Young's moduli in the parallel- and perpendicular-to-grain directions
 - b. Shear modulus in the board wide-face plane
 - c. Poisson's ratio in the board wide-face plane
 - d. Tensile strength parallel and perpendicular to grain
 - e. Shear strength parallel to grain
 - f. Mode I and Mode II fracture toughness in the wide-face plane
6. Knotwood properties, including
 - a. Young's moduli in the tangential and radial directions of the knot
 - b. Shear modulus in the wide-face knot plane

- c. Poisson's ratio in the wide-face knot plane
- d. Tensile strength perpendicular to grain of the knotwood; this is set to the perpendicular-to-grain tensile strength of the clear wood.

Clear-wood properties used in this research were established based upon the small clear-wood tests described previously. A single, presumably average, set of clear-wood strength and stiffness properties is used to characterize all the clear wood in a board. For the properties that were not directly measured, a prediction methodology was developed and employed from existing prediction equations and data (Bodig and Goodman 1973; Petterson and Bodig 1983; Schmidt 1987).

Knotwood properties were estimated based on work by Pugel (1980). He established that one set of elastic properties could be used to approximate the stiffness of most coniferous knotwood. We employed this assumption in our work in the absence of any other published research on knotwood properties.

Knot sizing and locating

Our investigation indicated that it is possible to use grain angles to locate and size knots (Badreddine 1988). We have achieved this objective through development of a computer algorithm within GASPP called KnotFinder, which analyzes grain angle data. The current version of this algorithm assumes, for simplicity, that each knot is elliptical in shape and that this ellipse can be defined by longitudinal and transverse diameters that coincide with the board geometric axes.

The only data required for knot sizing are the grain angles and the physical dimensions of the scanner data grid. The average and standard deviation of the grain angle values for each longitudinal scan line and the entire scanned portion of the board are calculated. These variational characteristics are compared to threshold values to establish knot boundaries. Specific details of these computations are undergoing verification for new data sets and will be published separately. Although the focus of this paper is not on automated knot definition, we will show that this capability provided sufficiently accurate knot sizes and locations for strength prediction.

Indeed, it is likely that grain angles provide a more accurate assessment of knot size than visual observations of the knot surface, at least for the influence of knot size on strength. To develop the KnotFinder algorithm, we had to proceed under the premise that carefully obtained visual measurements were sufficient and accurate representations of knot size and location. Only with this assumption and the visually obtained data could we establish the threshold grain variation parameters that aid in defining a knot.

Development of the knot location and sizing routine was conducted on 42 sets of grain angle data. These data sets were generated by scanning both wide faces of 21 Southern Pine and Douglas-fir 2 by 4's, of which the 14 tested single-knot boards were a subset. A visual examination of the 2 by 4's indicated 46 knots within the scan zones, of which 44 were detected with the KnotFinder routine. In both cases, the centers of the undetected knots were located off the edge of the board. The routine in its current stage of development is capable of detecting multiple knots, except when they are located along the same longitudinal scan lines. Although development of the routine focused on single knot situations, future research will establish the capability of the routine to detect and size multiple knots.

TABLE 2. *Difference between visual and predicted knot location and size.*

Knot location or size	Average difference between visual and predicted parameters* (in.)	Standard deviation (in.)
Knot location in transverse direction	0.07	0.19
Knot location in longitudinal direction	-0.11	0.52
Knot diameter in transverse direction	0.01	0.40
Knot diameter in longitudinal direction	0.06	0.41

* Predicted by KnotFinder routine.

Visual measurements were obtained for the center and the assumed transverse and longitudinal diameters of the 46 knots. Knots generally ranged from 1.0 to 2.0 in. in length and 0.75 to 2.0 in. in width. While a knot center can be readily identified, knot size as visually determined by the boundary between a knot and clear wood is a very subjective measurement.

In locating the centers of the knots, the KnotFinder routine compared closely to the visually measured parameters associated with each knot. The average and standard deviation of the differences in locating and sizing the knot relative to the visually measured parameters are shown in Table 2. Despite the subjective nature of visually sizing a knot, surprisingly close agreement between the visual measurements and the KnotFinder parameters is noted. This cannot be viewed as an independent verification, as the boards used for comparison were used in the development of the algorithm. However, this comparison shows the ability of the KnotFinder routine to account for variation in knot size and knot location within two species of structural lumber.

Mesh generation

Finite element representations or meshes are established as grids of nodal points that define the edges of finite elements. For this research, the nodal points associated with a mesh represent a surface or two-dimensional plane of a board. Since grain angle measurements are associated with one surface of the board, the question arises as to which surface or surfaces should be represented by the finite element mesh. We have found that grain angle readings associated with each wide face of a 2 by 4 are usually significantly different. In the mesh generator algorithm, we have included an option that considers grain angle measurements from both wide faces. An averaging scheme is employed that creates an idealized midthickness representation of the board (Juedes 1986). The averaging scheme works by aligning the knot centers on each face by shifting the grain angle grids relative to each other. The shift accommodates boards where the center of a knot is at different locations on each board surface. Once each face is aligned, the grain angle readings are averaged.

Nodal points are located along grainlines that are spaced at set distances along the base of the mesh. The grainlines are generated longitudinally by projecting them along the direction of the grain. Transverse lines are added, which, when combined with the longitudinal grainlines, create the sides of the finite elements. The finite element mesh thus reflects the actual average in-plane grain orientation of the board. A typical finite element mesh is shown in Fig. 2.

Once established, each finite element is assigned a grain angle at its centroid, based upon an interpolation of the measured angles. Grain angles within the knot

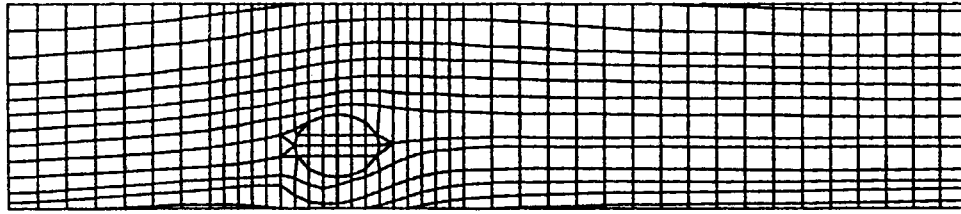


FIG. 2. Finite element 2 by 4 representation.

are set to a constant value of zero since special knot properties are used that reflect the out-of-plane orientation of those wood fibers.

Finite element and fracture analysis

Two-dimensional linear elastic behavior.—The constructed finite element mesh is analyzed assuming linear elastic material behavior, with only those stresses associated with the wide-face plane of lumber being nonzero. When cracks are not present, both clear wood and knotwood are modeled with a combination of eight-node quadrilateral and six-node triangular isoparametric finite elements (Cook 1981). Orthotropic properties are incorporated into the plane stress element formulation for the wide-face plane of the board.

The finite element solution provides displacements of each nodal point, from which the strains and stresses associated with each finite element are computed. These stresses are transformed from a global coordinate system to the local coordinate system for each element corresponding to the parallel- and perpendicular-to-grain directions. This allows us to compare element stresses with known wood strengths, which have been established experimentally or predicted for the parallel- and perpendicular-to-grain directions.

Fracture analysis.—Cracks are modeled as wood splits, which result during tensile failure of a board. Since seasoned wood generally exhibits brittle and linear elastic behavior under short duration tensile loads, the theory of linear elastic fracture mechanics has been considered appropriate for wood (Triboulet et al. 1984). According to this theory, crack propagation depends on the degree of stress intensity near the crack tip. The stress intensity factor is a parameter that indicates the intensity of stress in the material surrounding the crack tip for a given loading condition.

Two modes of fracture (consequently, two stress intensities) are prominent in lumber fracture and are modeled in this research. Mode I corresponds to opening-mode fracture usually resulting from severe tensile stresses perpendicular to grain, while Mode II fracture corresponds to sliding-mode fracture usually associated with high shear stresses.

Stress intensity factors are a function of the orthotropic material properties, the geometry of the wood member, and the loading. In this research, stress intensity factors are computed after determination of the crack opening displacements (COD). The COD are the displacements along the crack face measured relative to the crack tip. Reliable calculation of the COD is achieved through the use of quarter-point elements surrounding each crack tip (Freese and Tracey 1976). The COD are related to the stress intensity factors by orthotropic fracture equations.

Following the procedure described above, Mode I and Mode II stress intensity

factors are determined for the total number of cracks present in the wood member under consideration. There is no limit to the number of cracks that can be considered in a single analysis.

Failure and fracture theories.—The stresses and stress intensity factors computed by the model do not directly indicate local failure or fracture. These mathematical values must be interpreted with a set of rules that indicate critical combinations of stresses and stress intensity factors. In this research, “failure criteria” refer to the equations that are a function of stresses and wood strengths. In general, these equations indicate the combination of stresses and the load level necessary to cause localized failure or the initiation of fracture. “Fracture criteria” refer to the equations that relate Mode I and Mode II stress intensity factors to the corresponding wood fracture toughness values to indicate the load level necessary for a given crack to propagate.

Unfortunately, verified and generally accepted failure criteria have not been established for wood. This has resulted in part from the difficulty in establishing suitable specimens and tests with which to apply controlled biaxial stress states and collect the needed data. Data for establishing fracture criteria are also quite limited.

Based on our investigation of potentially applicable failure theories, the maximum stress failure theory has been incorporated into the model. The maximum stress failure theory predicts localized failure under increasing load when any of the three following conditions are satisfied:

$$\sigma_{\text{perp}}/\sigma_{u,\text{perp}} = 1 \quad (1)$$

$$\sigma_{\text{para}}/\sigma_{u,\text{para}} = 1 \quad (2)$$

$$(\tau)/(\tau_u) = 1 \quad (3)$$

where

σ_{perp} = tensile stress perpendicular to grain,

$\sigma_{u,\text{perp}}$ = uniaxial tensile strength perpendicular to grain,

σ_{para} = tensile stress parallel to grain,

$\sigma_{u,\text{para}}$ = uniaxial tensile strength parallel to grain,

τ = shear stress, and

τ_u = shear strength parallel to grain.

Adoption of these criteria does not imply that the maximum stress theory is totally suitable for this work. In fact, comparisons we have conducted with off-axis small clear-wood test data indicate that this theory is only a marginal predictor of failure (Juedes 1986). It is, however, the best predictor of failure available at this time, and in light of uncertainties in clear-wood properties, more complex theories cannot be justified.

Although fracture criteria have not been well established for wood, we have incorporated Wu's criterion in the GASPP model (Wu 1967). At least one investigation has indicated that Wu's criterion is appropriate for fracture in the tangential-longitudinal and radial-longitudinal plane of thin wood specimens (Mall et al. 1983). Wu's criterion assumes that the stress intensities corresponding to Mode I and Mode II interact as follows:

$$K_I/K_{IC} + (K_{II}/K_{IIC})^2 = 1 \quad (4)$$

where

- K_I = Mode I stress intensity factor,
- K_{IC} = critical Mode I stress intensity factor,
- K_{II} = Mode II stress intensity factor, and
- K_{IIC} = critical Mode II stress intensity factor.

Failure simulation through stepwise modeling.—With use of the maximum stress failure theory and computed element stresses, localized failures are identified according to failure modes corresponding to tension perpendicular to grain, tension parallel to grain, or shear. Tension perpendicular-to-grain or shear failures typically result in fracture along the wood grain. Experimental investigators have observed that fracture in wood will typically form and propagate along the grain (Anthony 1986; Pearson 1974; Pellicane 1980). This type of failure is modeled by separating the finite element mesh along the nearest grainline and using the special fracture finite elements to simulate the fracture that would occur in an actual test.

Tension parallel-to-grain failures are often splintering fractures crossing the grain. The resulting loss in stiffness parallel to grain is currently modeled by separating the finite element mesh across the grain and along the grain with a combination of horizontal and vertical cracks to simulate the splintering effect.

Local fractures as described are accumulated in the GASPP model by identifying local failure in each analysis step and by adjusting the finite element mesh for the next step of analysis to account for the identified local fracture. This means that a new mesh must be specified and generated each time a crack is added or extended. This procedure enables prediction of the load-displacement behavior of the board from initial load to ultimate collapse. An example of a load-displacement history resulting from the GASPP model is shown in Fig. 3. A plot of this type results when load is applied by pulling on the specimen ends at a prescribed rate of displacement. Stiffness loss resulting from modeled failure within the board can be identified. The points identified in Fig. 3 represent stable, equilibrium states of the modeled specimen. We have witnessed fracture occurring both in the modeled specimen and actual test generally anywhere between the points identified. Slow crack growth often occurs as load increases with displacement between points. The vertical dashed lines in Fig. 3 show the effect of certain critical fractures on the load-resisting capability of the specimen. These lines are dashed because the model cannot compute stable, equilibrium states in these regions, and it is likely that stable, equilibrium states do not occur in the actual test specimens in these regions. In an actual test, we have observed that critical fractures producing the vertical load drops will often be the result of sudden and simultaneous fracture events. In the model, all types of fracture are simulated by predicting individual crack growth under quasistatic conditions and accumulating the resulting damage in a step-by-step manner. In certain critical situations, the accumulated fractures from the model will also produce vertical load drops as shown in Fig. 3.

The peak load sustained by the modeled board is the predicted strength. Considerable variation can occur in the number of stepwise analyses needed to establish the strength, with from 5 to 50 steps needed. The analyst can often determine when the ultimate strength has been achieved by monitoring the amount of damage and loss in stiffness that has occurred in the modeled board.

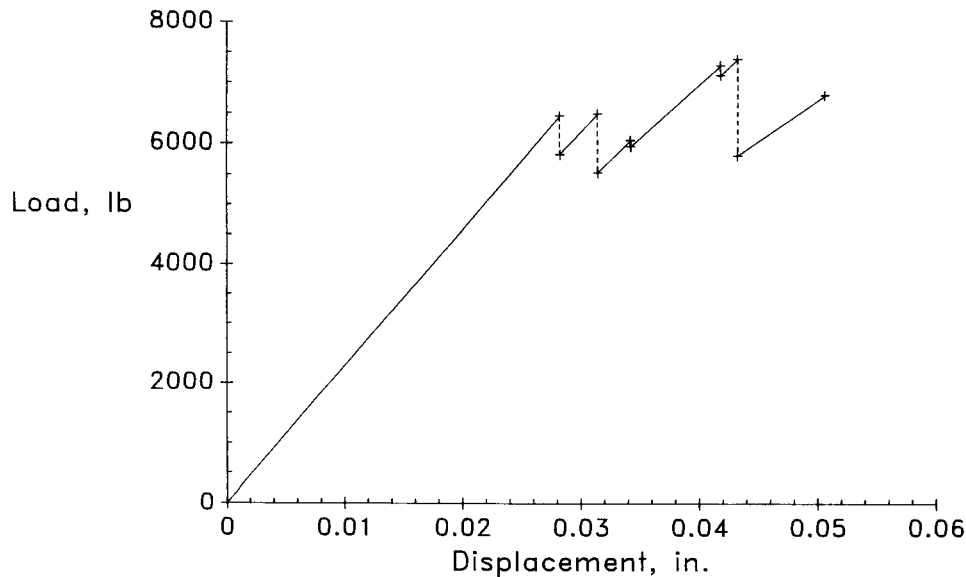


FIG. 3. Load and displacement resulting from step-wise failure modeling.

The stepwise analysis consisting of mesh regeneration and repeated finite element solutions is a computationally and manually intensive process. In an attempt to speed the modeling process, many analyses presented in this paper were conducted via satellite with a Cray supercomputer located in San Diego. Although nearly complete automation of this process is possible, it was inappropriate for this initial study.

MODEL PREDICTIONS AND VERIFICATION

Prediction of longitudinal modulus of elasticity

The effective moduli of elasticity of lumber sections containing knots were predicted with the GASPP model for the 2 by 4 population tested as part of this research. As mentioned earlier, longitudinal effective moduli of elasticity were measured with an extensometer over a 24-in. gauge length for the 14 test specimens. This gauge length covered wood containing the knot and associated grain deviation. Therefore, the longitudinal effective modulus measured in each case is a function of the clear-wood modulus, the amount of local grain deviation, and the modulus of the knotwood. The term effective modulus (E-eff) is used to distinguish this value from clear-wood stiffness properties. The measured E-eff values are listed in Table 3.

Effective modulus was predicted with the model by assigning the measured elastic properties for each board and generating the finite element mesh containing the measured local grain deviation. A uniform displacement was applied in a single analysis, and the resulting average applied stress at each end of the board segment was computed. A 16-in. length of each board was modeled in the computer. Thus, a predicted E-eff for a 16-in. span length was computed and compared to the measured E-eff from the 24-in. gauge length. Although the difference in

TABLE 3. Measured and predicted effective board moduli and measured clear-wood moduli.

Specimen	Knot type ^a	Modulus of elasticity (lb/in. ²)			Difference between measured and predicted moduli (percent)
		Measured		Predicted E-eff	
		E-eff ^b	Clear wood		
1	C	1,257,000	1,610,000	1,440,000	15
2	C	1,123,000	1,520,000	1,043,000	−7
3	C	1,981,000	2,580,000	2,190,000	11
4	O-C	1,571,000	1,990,000	1,618,000	3
5	O-C	1,790,000	2,440,000	1,930,000	8
6	O-C	1,514,000	1,520,000	1,313,000	−13
7	O-C	1,371,000	1,740,000	1,352,000	−1
8	E-1	1,371,000	2,090,000	1,594,000	16
9	E-1	1,333,000	1,340,000	1,091,000	−18
10	E-1	1,520,000	1,730,000	1,378,000	−9
11	E-1	1,429,000	1,810,000	1,502,000	5
12	E-2	1,285,000	1,490,000	1,259,000	−2
13	E-2	1,143,000	1,680,000	1,287,000	13
14	E-2	1,700,000	2,070,000	1,703,000	0

^a Knot types are defined in Table 1.^b E-eff is effective modulus.

gauge length will cause small changes in E-eff, this difference was ignored for the sake of simplicity. By converting the modeled uniform displacement to strain, E-eff was calculated as the average stress divided by the average strain. The predicted E-eff values are shown in Table 3 with associated measured clear-wood longitudinal modulus values. The percentage of difference between measured and predicted moduli was computed as the difference between the predicted E-eff and the measured E-eff divided by the measured E-eff. Predicted and measured E-eff values are compared in Fig. 4.

The predicted E-eff values were found to have a correlation coefficient of 0.88 with the measured values and an average absolute difference of 8%. The measured E-eff values and clear-wood moduli for boards 6 and 9 were virtually the same. We would expect the knot to have a greater stiffness-reducing effect than indicated by these values. Based upon this observation, we believe the quality of our estimate of the average clear-wood stiffness for each board is the primary source of difference between measured and predicted E-eff values in Table 3.

Prediction of strength

By employing the stepwise failure modeling process discussed earlier, the ultimate strength value for each of the 14 boards was predicted. As discussed earlier, this sample included Southern Pine and Douglas-fir lumber with a single prominent defect of varying sizes and locations within the cross section. The results from GASPP modeling and tension testing are summarized in Table 4 and Fig. 5. The absolute average error in predicting strength was 12%, with a correlation coefficient of 0.86. One prediction (for specimen 9) was significantly worse than the others. We could find no reason why this particular board had considerably less strength than predicted. We presume that an undetected defect or zone of damage accounted for the unexpected low strength. In the absence of this poor prediction, the correlation coefficient between predicted and measured strengths is 0.96.

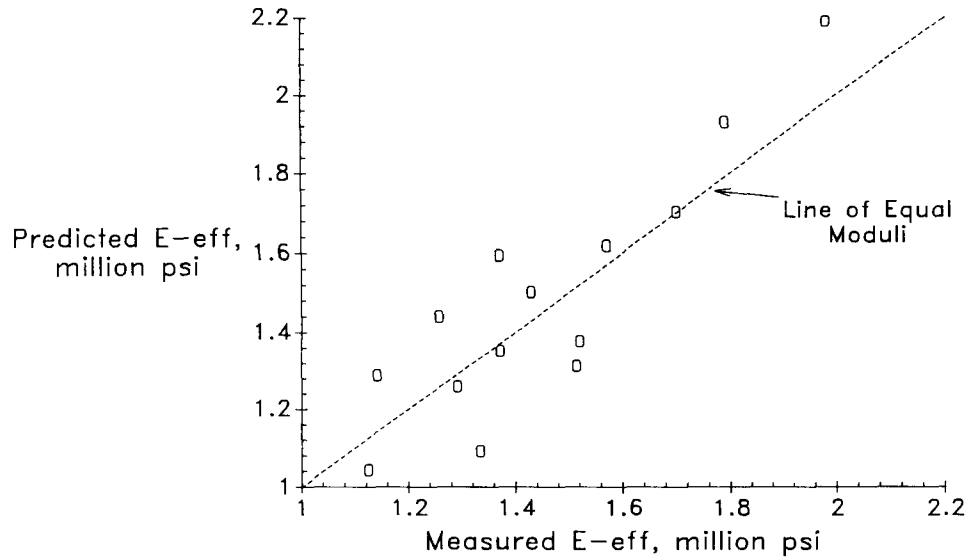


FIG. 4. Measured and predicted longitudinal effective moduli (E-eff) of elasticity for fourteen 2 by 4 lumber samples.

DISCUSSION

Success in predicting strength with the GASPP model depended on two key components in our process. The first component was accurate calculation of local stresses, and the second, accurate assessment of the severity of local stresses with local failure and fracture criteria. Accurate stress calculation is dependent on accurate elastic property information, sufficient mesh fineness, and loading conditions that accurately reflect the load conditions imposed by the testing machine.

Small clear-wood tests indicated the average elastic properties within the board.

TABLE 4. Measured and predicted board tensile strength.

Specimen	Knot type	Tensile strength (lb)		Difference between measured and predicted strength (percent)
		Measured	Predicted	
1	C	30,060	25,300	-16
2	C	13,400	11,130	-17
3	C	34,200	34,910	2
4	O-C	26,920	25,180	-6
5	O-C	17,420	18,900	8
6	O-C	19,460	19,740	1
7	O-C	15,700	16,820	7
8	E-1	15,440	16,010	4
9	E-1	14,020	23,260	66
10	E-1	20,020	16,590	-17
11	E-1	21,520	20,600	-4
12	E-2	18,600	16,440	-12
13	E-2	17,080	17,260	1
14	E-2	24,280	24,500	2

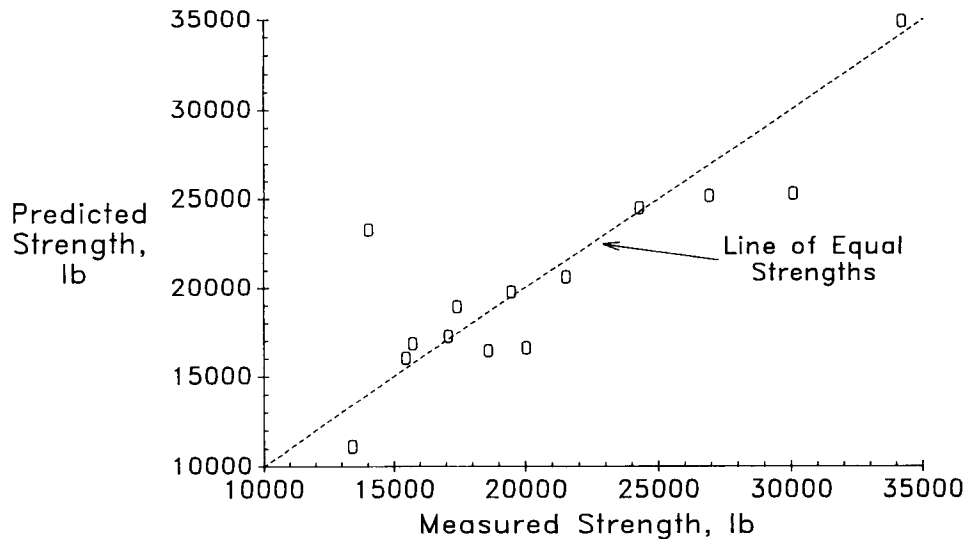


FIG. 5. Measured and predicted tensile strength for 14 lumber samples.

The elastic properties are important since they directly influence the magnitude of stress in each element. The available supply of clear wood for each specimen resulted in only two test replicates per board for each measured clear-wood property. These two tests indicated great variability in the clear-wood elastic and strength properties within an individual board, and this small number of replicates consequently provided a rather crude indication of the average board properties. It should be noted that the resulting estimates of average clear-wood properties were sufficient, however, to provide reasonable predictions of board strength. This is important since in both research and application it will be difficult to readily obtain more accurate information on average properties.

Mesh fineness (the concentration of finite elements in an area) proved to be of major concern in our modeling. Our investigation indicated that great care was necessary in ensuring that sufficiently small elements were used in regions of local failure. Insufficient mesh fineness leads to gross averaging of steep grain angle gradients and poor accuracy in stress calculation.

Accurate simulation of the testing machine loading conditions was necessary to achieve accurate calculations of stress. Restraint of the modeled specimen such that rotations were restricted was necessary to reflect the conditions imposed by the tension machine. For edge knots, we found that it was necessary to consider nearly the full board length between machine grips to accurately reflect the bending resulting from the eccentric knot. For centerline knots, shorter board segments could be analyzed successfully. A different tension loading apparatus would likely result in different measured and predicted tensile strengths.

The second component of our modeling process, interpretation of stresses with failure and fracture criteria, has been discussed. The lack of a proven biaxial failure criterion for clear wood is a limitation to achieving greater accuracy with the developed GASPP model.

Our simulations indicated that there is considerable variation in the manner

in which boards fail. Centerline-knot boards tend to experience their first fracture relatively close to ultimate strength, whereas edge-knot boards experience first fracture at loads well below ultimate strength. In many cases, small, seemingly inconsequential fractures occur very near the knot and are followed by major fractures away from the knot, which determine the board strength. In nearly all cases, fracture was a continuous process leading to a state of stress that determined the board strength. Our model indicated that it would be difficult to predetermine this state of stress without first accounting for the local fracture that occurs.

Based upon our results, surface grain angle appears to provide sufficient information on grain orientation to predict tensile strength. However, our experience suggests that dive may be critical in certain situations. Knot types corresponding to E-1 (see Table 1) contain a small amount of clear wood between the knot and the board edge on one wide-face surface. The size and integrity of this small region of clear wood can dramatically influence the strength of boards of this type. It is possible that our surface grain angle model overpredicts the integrity of this wood located so near the knot and that some adjustment should be made for the possibility of steep dive angles in this region. This concept may explain the poor strength prediction for specimen 9.

CONCLUDING REMARKS

A finite element and fracture mechanics model has been developed to predict the tensile strength of lumber boards containing a single face knot. The primary input to the model is a set of local surface grain angles for each wide face of a board and estimates of average clear-wood properties. The model is based upon principles of mechanics and does not depend upon any empirical adjustment factors. The model simulates the failure process that occurs within lumber subject to tension, and it thereby provides insight on the failure of wood with defects in addition to predicting strength. Verification has shown that model predictions of strength correlate with measured strengths by a correlation coefficient of 0.86. This strength prediction capability is demonstrated for a variety of knot sizes and locations within the board cross section and includes consideration of two structural wood species.

Based upon our experience, we believe there is great potential to extend and apply this research. Future research should be directed toward multiple knot situations, other wood species, especially hardwoods, other loading modes, such as bending, and consideration of the effect of diving grain angles. Such work will continue to enhance our understanding of failure mechanisms associated with structural lumber.

We have attempted to establish a strong foundation from which improved grading methods for lumber can be developed. Future work should also include developing simplified models based upon knowledge gained with GASPP. A simplified model based upon the research discussed here would enable industrial real-time predictions of board strength and would allow new options in the way lumber is graded and used.

ACKNOWLEDGMENTS

The authors appreciate the contributions of former research assistants Brian Juedes, Mark Schmidt, and Loei Baddredine. Technical assistance of Friend

Bechtel and James Allen of Metriguard, Inc., during scanning is appreciated. Financial support of the Forest Products Laboratory and computational support of the National Science Foundation through the San Diego Supercomputer Center are gratefully acknowledged.

REFERENCES

- ASCE. 1984. Structural wood research—State-of-the-art and research needs. R. Y. Itani and K. F. Faherty, eds. American Society of Civil Engineers, New York.
- ASTM. 1987a. Standard methods of static tests of timbers in structural sizes. American Society of Testing and Materials, Method D 198-84.
- . 1987b. Standard methods of testing small clear specimens of timber. American Society of Testing and Materials, Method D 143-83.
- ANDERSON, E. A., AND A. KOEHLER. 1955. Instruments for rapidly measuring slope of grain in lumber. USDA Forest Serv., Forest Prod. Lab. Rep. 1592.
- ANTHONY, R. W. 1986. Experimental data for the tension behavior of Douglas-fir with defects. M.S. thesis, Colorado State University, Ft. Collins.
- BADREDDINE, L. 1988. Supporting studies and tests for modeling lumber in tension. M.S. independent study report, Dept. of Civil and Environmental Engineering, University of Wisconsin, Madison.
- BECHTEL, F. K., AND J. R. ALLEN. 1987. Methods of implementing grain angle measurements in the machine stress rating process. Sixth Symposium on Nondestructive Testing of Wood. Washington State University, Pullman. September. Pp. 303-353.
- BOATRIGHT, S. W. J., AND G. G. GARRETT. 1979. The effect of knots on the fracture strength of wood II. A comparative study of the methods of assessment, and comments on the application of fracture mechanics to structural timber. *Holzforschung* 33:73-77.
- BODIG, J., AND J. R. GOODMAN. 1973. Prediction of elastic parameters for wood. *Wood Sci.* 5(4): 249-264.
- COOK, R. D. 1981. Concepts and applications of finite element analysis. John Wiley and Sons, Inc., New York.
- CRAMER, S. M. 1981. A stress analysis model for wood structural members. M.S. thesis, Colorado State University, Ft. Collins.
- , AND J. R. GOODMAN. 1986. Failure modeling: A basis for strength prediction of lumber. *Wood Fiber Sci.* 18(3):446-459.
- DABHOLKAR, A. 1980. Finite element analysis of wood with knots and cross grain. Ph.D. dissertation, Colorado State University, Ft. Collins.
- FREESE, C. E., AND D. M. TRACEY. 1976. The natural isoparametric triangle versus collapsed quadrilateral for elastic crack analysis. *Int. J. Fracture* 12:767-770.
- GREEN, A. E. 1945. Stress systems in anisotropic plates. *Proceedings of the Royal Society of London, PRSLA*, Vol. 184A.
- JUEDES, B. J. 1986. Failure modeling of wood tensile members. M.S. independent study report, University of Wisconsin, Madison.
- KOEHLER, A. 1955. Guide to determining slope of grain in lumber and veneer. USDA Forest Serv., Forest Prod. Lab. Rep. 1585.
- MALL, S., J. E. MURPHY, AND J. E. SHOTTAFFER. 1983. Criterion for mixed mode fracture in wood. *J. Eng. Mech. ASCE* 109(3):680-690.
- MCDONALD, K. A., AND B. A. BENDTSEN. 1986. Measuring localized slope of grain by electrical capacitance. *Forest Prod. J.* 23(5):75-78.
- , S. M. CRAMER, AND B. A. BENDTSEN. 1987. Research progress in modeling tensile strength of lumber from localized slope of grain. Sixth Symposium on the Destructive Testing of Wood. Washington State University, Pullman.
- MCLAUCHLAN, T. A., AND D. J. KUSEC. 1978. Continuous non-contact slope-of-grain detection. Fourth Symposium on Nondestructive Testing of Wood, Washington State University, Pullman. Pp. 67-76.
- , J. A. NORTON, AND D. J. KUSEC. 1973. Slope-of-grain indicator. *Forest Prod. J.* 23(5): 50-55.
- PEARSON, R. G., 1974. Application of fracture mechanics to the study of tensile strength of structural lumber. *Holzforschung* 28(1):11-19.

- PELLICANE, P. J. 1980. Ultimate tensile strength analysis of wood. Ph.D. dissertation, Colorado State University, Ft. Collins.
- PETTERSON, R. W., AND J. BODIG. 1983. Prediction of fracture toughness of conifers. *Wood Fiber Sci.* 15(4):302-316.
- PHILLIPS, G. E., J. BODIG, AND J. R. GOODMAN. 1981. Flow-grain analogy. *Wood Sci.* 14(2):55-64.
- PUGEL, A. D. 1980. Evaluation of selected mechanical properties of coniferous knotwood. M.S. thesis, Colorado State University, Ft. Collins.
- . 1986. Fracture mechanics-based failure criterion for wood. Ph.D. thesis, Colorado State University, Ft. Collins.
- SCHMIDT, M. K. 1987. Modeling considerations for predicting the tensile behavior of lumber. M.S. independent study report, University of Wisconsin, Madison.
- SOEST, J. F. 1987. Applications of optical measurement of slope of grain. Sixth Symposium on Nondestructive Testing of Wood, Washington State University, Pullman.
- TANG, R. C. 1984. Stress concentration around knots in laminated beams. *Wood Fiber Sci.* 16(1): 55-71.
- TRIBOULET, P., P. JODIN, AND G. PLUVINAGE. 1984. Validity of fracture mechanics concepts applied to wood by finite element calculation. *Wood Sci. Technol.* 18:51-58.
- WU, E. M. 1967. Application of fracture mechanics to orthotropic plates. *J. Appl. Mech.* 12:967-974.
- ZANDBERGS, J. G., AND F. W. SMITH. 1988. Finite element fracture predictions for wood with knots and cross grain. *Wood Fiber Sci.* 20(1):97-106.